Physical Modeling of the Effect of *Rhizophora mangle* and *Avicennia germinans* on Wave Runup

Samantha Chan
Naval Architecture and Ocean Engineering
United States Naval Academy
Annapolis, USA
samanthachan026@gmail.com

Tori Tomiczek, PhD
Naval Architecture and Ocean Engineering
United States Naval Academy
Annapolis, USA
vjohnson@usna.edu

Anna Wargula, PhD
Naval Architecture and Ocean Engineering
United States Naval Academy
Annapolis, USA
wargula@usna.edu

***Abstract* – This project examines mangrove forests as resilient, sustainable, and non-invasive shoreline protection in subtropical and tropical areas. Hydrodynamic data were collected from idealized *Rhizophora mangle* and *Avicennia germinans* forest models. The data were analyzed to identify trends between the heterogeneity of a mangrove forest and wave runup extents. Different species of mangroves have a distinctive root system which attributes to different coastal protection abilities. Shorter wave periods were most affected by mangrove configurations tested. Configurations dominated by *R. mangle* models resulted in overall smaller runup extents compared to configurations dominated by *A. germinans* models for the same wave conditions.**

I. Introduction

The motivation for finding a resilient and sustainable shoreline protection is that as sea levels and global temperatures rise, coastal communities become more vulnerable to inundation and wave action during severe storms. Mangroves have been promoted as alternatives to manmade shoreline protection because mangroves are a native species in subtropcial and tropcial regions. Hardened shoreline protection systems may not always be resilient solutions, because in addition to reducing habitats, they are not naturally adaptable in a changing climate. In addition to potential shoreline protection, mangroves provide cobenefits such as carbon sequestration, habitat, and nurseries, and they have been shown to recover after damage in a storm.

Previous studies conducted laboratory tests, which focused on homogeneous forests and generally considered only wave height attenuation through the forest [1-3]. This project examines effects of forest heterogeneity on wave runup extents. Wave runup and runup extents are important for designing near-shore infrastructure such as roads and buildings, mitigating erosion, and protecting inland areas during storm surge events. The two species explored in this project were *Rhizopora mangle* and *Avicennia germinans*.

A. Rhizophora mangle

R. mangle (red mangrove) is found primarily in the Americas in the subtropical and tropical regions [4]. Growing an average of 5 to 10 meters tall, *R. mangle* is known for its distinctive above-ground prop-root system shown in Fig. 1. The prop roots are multifunctional, anchoring the tree and supporting its growth in oxygen-poor environments; in addition, they serve as a habitat and nursey to a variety of species.

Fig. 1. *Rhizophora mangle*

B. Avicennia germinans

A. germinans (black mangrove) is found primarily in southern Florida; it can also be found in the northern part of the Gulf Coast. It typically grows inland of *R. mangle* [5]. Reaching an average height of 15 meters, *A. germinans* is known for its distinctive snorkel-root system shown in Fig. 2. The snorkel roots serve as the breathing mechanism for the species.

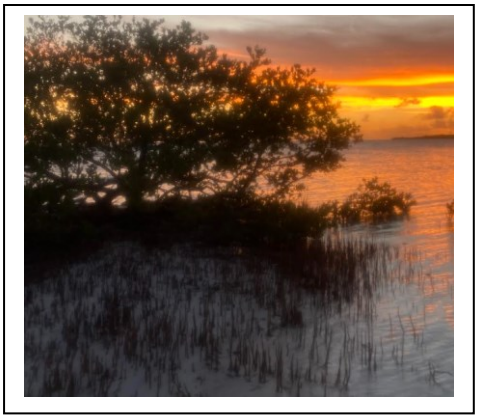

Fig. 2. *Avicennia germinans*

II. Methodology

A. Model

To investigate the effects of *R. mangle* and *A. germinans* and forest heterogeneity on wave runup extents, a physical model was constructed in the 10.7 m by 1.0 m Sediment Tank, located in the Coastal Laboratory at the United States Naval Academy. The beach slope capability of the sediment tank is 1:10 (vertical-to-horizontal), which is equivalent to approximately 5.7 degrees, comparable to beach slopes in the Florida Keys, which range 4 to 6 degrees [6]. Upon generation, waves traveled 4.92 m to the onset of the 1:10 slope. The slope begins at x = 4.92 m where x is the distance from the wavemaker. A profile of the sediment tank is shown in Fig. 3, where x is the distance from the side opposite of the wavemaker. Fig. 4 shows a photograph of the sediment tank showing an oblique view from the beach toward the wavemaker, with the profile, shown as the yellow line in Fig. 3, marked in blue tape.

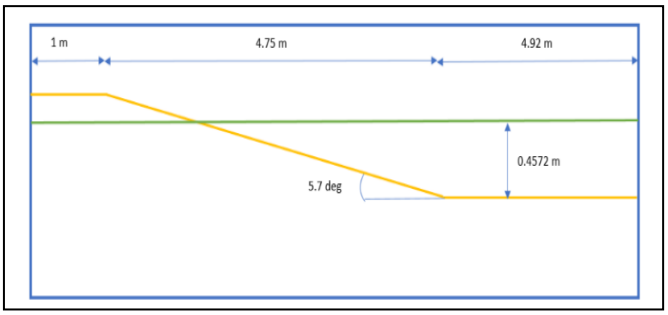

Fig. 3. Profile View of Sediment Tank

Fig. 4. Photograph of Sediment Flume with 1:10 Slope Marked in Blue Tape

The geometric scale of the model mangrove trunk-root system was 1:4. The dimensions of the entire forest were 2 m (cross-shore) by 1 m (along-shore), and the forest area was divided into eighteen identical sections to allow for placement of either *R. mangle* or *A. germinans* mangrove models. A grid system was used in the sediment tank to uniformly interchange the mangrove species model to vary the stem density of *R. mangle* or *A. germinans*. The sand at the bottom of the sediment tank was used to anchor the stems and prop roots or snorkel roots in place. Fig. 5 illustrates the 6 x 3 grid system design for the model mangrove forest with a 100% *R. mangle* configuration.

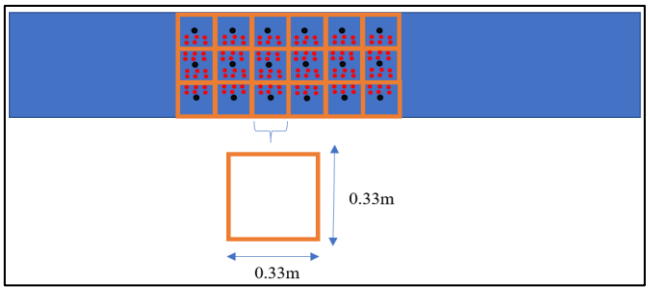

Fig. 5. Plan View Diagram of Sediment Tank with 100% *R. mangle* Mangrove Forest Configuration Showing Placement of Trunks (Black Circles) and Prop Roots (Orange Circles)

A total of 36 mangroves (18 *R. mangle* and 18 *A. germinans*) were constructed. Based on the grid system for the forest planform (Fig. 5), the maximum number of *R. mangle* mangroves tested at once was 18, and the maximum number of *A. germinans* mangroves tested at once was 18. The 6 x 3 grid resulted in a stem density of 9 stems/m^2 at reduced scale, which is equivalent to approximately 0.5 stems/m^2 at full scale. A mangrove forest prototype density of approximately 0.5 stems/m^2 falls between the "low" and "high" density cases conducted in Kelty et al. [1]. The prototype and reduced scale tree dimensions are listed in Table 1. An identical trunk diameter and height was assumed for both *R. mangle* and *A. germinans*. The diameters and heights of the prop and snorkel roots were determined based on average mature forest values [6-8]. The materials for mangrove components are selected similar to the 1:16 scale model by Tomiczek et al. [8] as presented in Table 2.

TABLE I. Dimensions of Mangrove Components

	Prototype Scale cm (in)	Reduced Scale cm (in)
Trunk Diameter	11.43 (4.5)	2.86 (1.13)
R. Mangle Root Diameter	2.86 (1.13)	0.72 (0.28)
R. Mangle Root Height	210 (82.68)	52.5 (20.67)
A. Germinans Root Diameter	0.80 (0.31)	0.25 (0.10)
A. Germinans Root Height	20.32 (8)	5.08 (2.00)

TABLE II. Materials for Model Mangrove Components

Mangrove Part	Prototype Material
Trunk	PVC Pipe
Prop Root	Wood Dowel
Snorkel Root	Galvanized Steel Wire

The number of snorkel roots per *A. germinans* was 26. The number of prop roots per *R. mangle* was 12. The mangrove cells adjacent to the side walls of the sediment tank (Fig. 5) were constructed as "half-trees," with half of the roots of either respective mangrove model. Therefore, the number of snorkel roots per *A. germinans* along the wall of the sediment tank was 13 and the number of prop roots per *R. mangle* along the wall of the sediment tank was 6. A total of 144 prop roots for the 18 total *R. mangle* were constructed. A total of 312 snorkel roots for the 18 total *A. germinans* were constructed. The height of every trunk was 0.4572 m, and tree canopies were conservatively neglected following the methods of previous studies [1-3], assuming that trees were not submerged by hydrodynamic conditions.

The trunk diameter at breast height (*DBH*) for the prototype-scale *R. mangle* model was approximately 0.11 m. Based on the *Rhizophora* prop root model proposed by Ohira et al. [9], the root height of the highest primary root ($H_{R_{max}}$), number of primary roots (N), and the root spread distance (x_2) were calculated as listed in Table 3.

TABLE III. *R. MANGLE* MEASUREMENTS

	Actual Size (cm)	Reduced Scale cm (in)
DBH	11	2.75 (1.08)
$H_{R_{max}}$	133.16	33.29 (13.11)
x_2	192.82	48.20 (18.98)
N	12.76	--

B. Testing

Four different forest configurations were tested to investigate the effectiveness of no forest, a *R. mangle* forest, an *A. germinans* forest, and a heterogeneous forest comprising 50% *R. mangle* and 50% *A. germinans*. The mangrove species composition for each configuration tested are provided in Table 4. The configuration without a forest was referred to as the baseline configuration for which to compare wave runup extents measured for all other forest configurations. The water depth for all the tests was held constant at 0.4572 m.

Regular waves were generated through each configuration; wave characteristics are presented in Table 5 and considered a constant wave amplitude for two wave periods. A wave gauge positioned at x = 4.26 m sampled water surface elevations at a frequency of 50 Hz. The mean and standard deviation for wave condition 2 (Table 5) was found to determine the reliability of the wavemaker input to output. For wave condition 2, the mean and standard deviation of the measured wave height were 0.025 m and 0.00089 m, respectively, for three trials. In addition, the mean and standard deviation of the measured wave period were 1.007 s and 0.0008 s, respectively, for this wave condition. Each forest configuration is shown in Fig. 6, 7, and 8, with photographs taken looking toward the wavemaker from the inland edge of the forest.

TABLE IV. TESTING CONFIGURATIONS SHOWING MANGROVE-TYPE COMPOSITION

	R. mangle	*A. germinans*
Baseline (No Forest)	*0%*	*0%*
Configuration 1	100%	0%
Configuration 2	50%	50%
Configuration 3	0%	100%

TABLE V. WAVE CHARACTERISTICS

Wave Condition	Amplitude m (in)	Frequency (Hz)	Period (s)
1	0.03 (1.18)	1.8	0.56
2	0.03 (1.18)	1	1

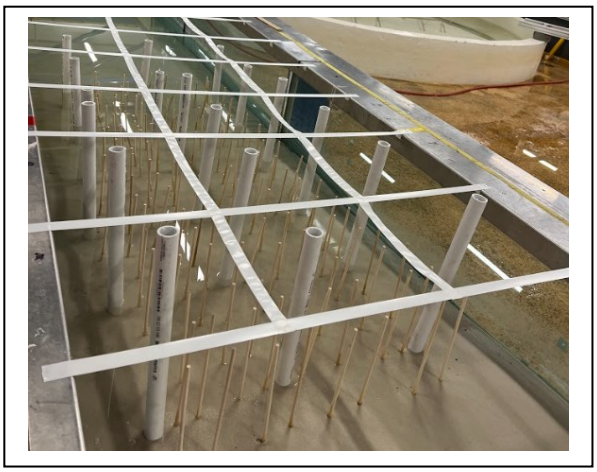

Fig. 6. Photograph Showing 100% *R. mangle*, 0% *A. germinans* Mangrove Forest Test Configuration

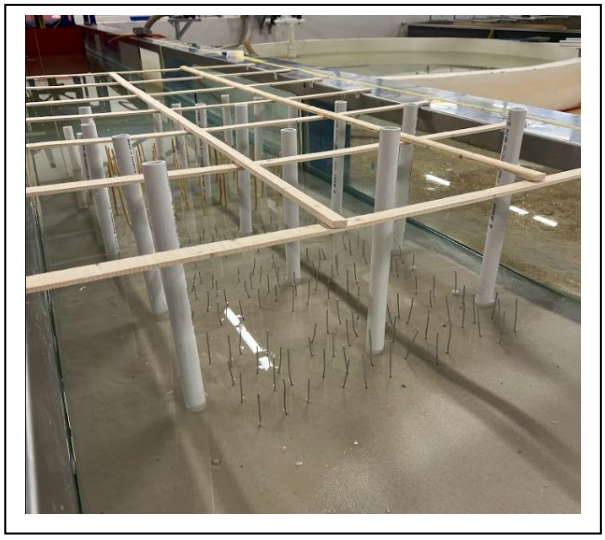

Fig. 7. Photograph Showing 50% *R. mangle*, 50% *A. germinans* Mangrove Forest Test Configuration

Fig. 8. Photograph Showing 0% *R. mangle*, 100% *A. germinans* Mangrove Forest Test Configuration

The method for determining wave runup extents is illustrated in Fig. 9. Each trial was video-taped from an aerial perspective, and a meter stick was placed at a fixed location for each trial. The maximum runup extents, defined as the maximum length along the meter stick reached by the water, was taken based on the videos to the nearest 1.27 cm (0.5 inch). Each trial was 10 seconds long; there were 18 waves for wave condition 1 and 10 waves for wave condition 2.

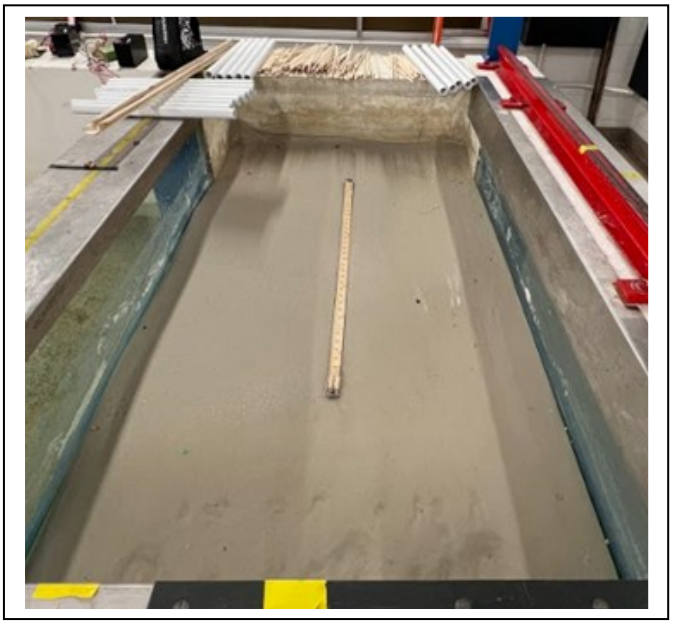

Fig. 9. Test Runup Determination Method

III. RESULTS

Table 6 summarizes test results for the baseline and various mangrove configurations. In the table, R stands for the runup extent in centimeters, T is the wave period in seconds, and S is standard deviation of the runup extent centimeters.

TABLE VI. SUMMARY OF TEST RESULTS

Config.	T = 1 sec				T = 0.56 sec			
	Baseline		***Mangrove Config.***		***Baseline***		***Mangrove Config.***	
	$\bar{R}$	S_R	$\bar{R}$	S_R	$\bar{R}$	S_R	$\bar{R}$	S_R
100% *Avic.*	91.44	--	91.44	0	6.35	--	5.92	1.47
50% *Avic.*, 50% *Rhizo.*	55.88	--	51.64	5.28	22.86	--	22.86	0
100% *Rhizo.*	30.48	--	26.67	1.27	10.16	--	5.92	1.47

The mean and standard deviation runup extent were calculated for each configuration to determine the effect of each mangrove forest configuration on wave runup extent compared to the baseline configuration. To assess the effect of *A. germinans* and *R. mangle* mangrove forest composition on wave runup extent, the total volume of stems and roots for each configuration was calculated. This volume was divided by the maximum possible occupiable volume of the trunk, computed as the plan area of the forest footprint times the height of the trunk. Wave runup extent was plotted against this relative forest volume in Fig. 10.

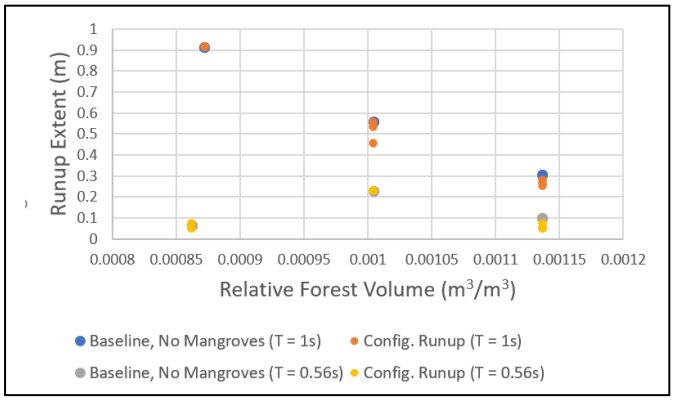

Fig. 10. Wave Runup Extent (m) vs. Relative Mangrove Forest Volume (m^3/m^3)

To further investigate the effect of each *A. germinans* and *R. mangle* mangrove forest configuration with respect to incident wave conditions on wave runup extents, the total volume of the stems and roots for each configuration was divided by the square of the mean measured incident wave height (H) times the incident wavelength (L) calculated using linear wave theory. The measured wave runup extents was plotted against this parameter as shown in Fig. 11.

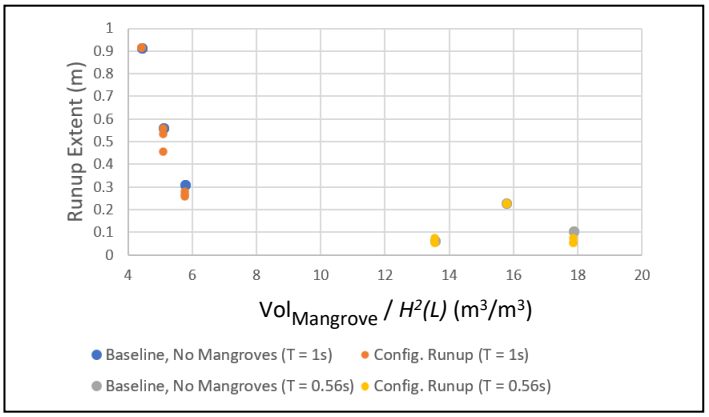

Fig. 11. Wave runup extent (m) vs. mangrove volume normalized by incident wave conditions (H^2L)

IV. CONCLUSION

As suggested by Figs. 10 and 11, the runup extents caused by waves with shorter periods (smaller wavelengths) were most affected by the mangrove configurations. Mangrove configurations tested for wave condition 1 (T = 0.56 s) experienced smaller runup extents compared to runup extents measured for the same configuration subject to wave conditions with T = 1 s. Shorter period waves resulted in overall smaller runup extents for the same mangrove configurations, compared to those observed for longer wave periods.

Because the sediment tank bottom was composed of sand, an important observation during testing was that trials conducted with *R. mangle*-dominated mangrove configurations (Configuration 1, Table 4) experienced less bathymetry changes compared to bathymetry changes observed for *A. germinans*-dominated mangrove configurations (Configuration 3, Table 4). The change in bathymetry was noted after each mangrove configuration and determined qualitatively by assessing the deviation from the initial slope marked with blue tape shown in Fig. 4. Tests were conducted for shorter periods of time to try to limit bathymetry change, and raked between each configuration to ensure a constant starting point.

Relative *R. mangle* composition within the mangrove configurations tested was directly related to the overall runup extents. For T = 1 sec, a negative relationship was observed between *R. mangle* composition and mean runup extents, with greater composition of *R. mangle* resulting in smaller runup extents. This result suggests that *R. mangle* may be more effective at decreasing wave runup extents compared to *A. germinans*, owing to the greater volume occupied by the mangrove biomass. Additional tests are needed to verify this trend.

Future work to expand on this project includes (1) determining the importance and influence of beach slope in affecting wave runup extents, (2) determining the influence of mangroves on sediment transport, accretion, and quantifiable beach slope change, (3) exploring a greater range of wave heights and periods and their relative contribution to wave runup extents in the presence of mangroves, and (4) considering other configurations and species of heterogeneous vegetation. With additional testing, better understanding of mangrove performance can help to better inform the appropriate implementation of these systems as coastal protection.

ACKNOWLEDGMENT

The authors thank Dr. James Gose and Mr. John Balano for their expertise and support in data collection, which was instrumental to the success of the project This project was supported by funding from the U.S. Army Corps of Engineers and National Science Foundation CBET Grant #2110262. Any opinions, findings, and conclusions or recommendations expressed in this material are those of the author(s) and do not necessarily reflect the views of the United States Naval Academy, U.S. Army Corps of Engineers, or the National Science Foundation.

REFERENCES

[1] Kelty K, Tomiczek T, Cox DT, Lomonaco P and Mitchell W (2022) Prototype-Scale Physical Model of Wave Attenuation Through a Mangrove Forest of Moderate Cross-Shore Thickness: LiDAR-Based Characterization and Reynolds Scaling for Engineering With Nature. Front. Mar. Sci. 8:780946. doi: 10.3389/fmars.2021.780946

[2] John Ragan, and Richard Smosna. "Sedimentary Characteristics of Low-Energy Carbonate Beaches, Florida Keys." Journal of Coastal Research, vol. 3, no. 1, 1987, pp. 17, http://www.jstor.org/stable/4297244. Accessed 25 Apr. 2022.

[3] Snedaker S, Jimenez J, Brown M (1981) Anomalous Aerial Roots in *Avicennia Germinans* (L.) L. in Florida and Costa Rica. Newfound Harbor Marine Institute. Bulletin of Marine Science, 31(2): 467-470.

[4] "*Rhizophora mangle* (red mangrove)." CABI International. 2022. https://www.cabi.org/isc/datasheet/47509

[5] "Avicennia germnans." Lady Bird Johnson Wildflower Center. 2016. https://www.wildflower.org/plants/result.php?id_plant=AVGE

[6] John Ragan, and Richard Smosna. "Sedimentary Characteristics of Low-Energy Carbonate Beaches, Florida Keys." Journal of Coastal Research, vol. 3, no. 1, 1987, pp. 17, http://www.jstor.org/stable/4297244. Accessed 25 Apr. 2022.

[7] Snedaker S, Jimenez J, Brown M (1981) Anomalous Aerial Roots in *Avicennia Germinans* (L.) L. in Florida and Costa Rica. Newfound Harbor Marine Institute. Bulletin of Marine Science, 31(2): 467-470.

[8] Tomiczek, T., Wargula, A., Lomonaco, P., Goodwin, S. Cox, D.T., Kennedy, A.B., Lynett, P. 2020. Physical model investigation of mid-scale mangrove effects on flow hydrodynamics and pressures and loads in the built environment. Coastal Engineering, 162 (2020), DOI: https://doi.org/10.1016/j.coastaleng.2020.103791.

[9] Ohira, W., Honda, K., Nagai M., Ratansuwan A. 2013. Mangrove silt root moephology modeling for estimating hydraulic drag in tsunami inundation simulation. Springer. DOI 10.1007/s00468-012-0782-8.